

Transient Sorption and Desorption Studies of Cyclopropane and Propylene with Cs/NaX and Ni/NaX Zeolites

ANGELOS M. EFSTATHIOU,* STEVEN L. SUIB,*^{†,1} AND CARROLL O. BENNETT*

*Departments of *Chemical Engineering and †Chemistry, University of Connecticut, Storrs, Connecticut 06269-3060*

Received May 22, 1991; revised January 6, 1992

Transient diffusion and sorption experiments of cyclopropane and propylene in Cs⁺ and Ni²⁺ ion-exchanged Zeolites X in a flow microreactor reveal that the nature of the diluent gas affects the kinetics of intracrystalline mass transport of these molecules in the zeolite. The rate of intracrystalline mass transport and the equilibrium uptake are strongly dependent on temperature. The results indicate that cyclopropane does not react with either Cs⁺ or Ni²⁺ ion-exchanged Zeolites X in the range 40–240°C to give other gas-phase products. For Cs/NaX the enthalpy of sorption for cyclopropane at loadings approaching zero is –8.8 kcal/mol, and the entropy of sorption is –31.2 cal/mol-K. For Ni/NaX the enthalpy of sorption for both cyclopropane and propylene is –9.1 kcal/mol, and the corresponding values for the entropy of sorption are –30.8 and –29.8 cal/mol-K.

© 1992 Academic Press, Inc.

INTRODUCTION

The large amount of work in zeolitic diffusion and sorption shows that diffusion and sorption rates of different molecules are sensitive to the (a) nature of the cation in the zeolite (charge, ionic radii), (b) position of the cation in the framework (effective window opening), (c) degree of ion exchange, and (d) molecular occupancy (number of molecules per unit cell) in the zeolite crystal (*1–3*). A thorough understanding of the effect of each of these inherent zeolitic parameters on diffusion and sorption processes would certainly improve the practical applications of zeolite materials.

The transient sorption of *c*-C₃H₆ in H₂, He, and Ar diluent gases in the NaX zeolite has been studied (*4*). The nature of diluent gas used in the *c*-C₃H₆ mixture affected the kinetics of intracrystalline mass transport of *c*-C₃H₆ in the zeolite. It was suggested that this phenomenon is due to collisional effects that influence the diffusion of *c*-C₃H₆ from one cavity to the next one, rather than a

competition for sites between the inert diluent gas and *c*-C₃H₆ (*4*).

In our recent work on cyclopropane and propylene transient diffusion, sorption, and reaction with Eu³⁺ ion-exchanged Zeolite X, it was found that this zeolite promotes the isomerization reaction of cyclopropane to propylene at temperatures higher than 80°C (*5*). In addition, propylene sorption in Eu/NaX was larger than that in NaX (*5*). These results were due to the presence of Brønsted acid sites formed after dehydration of the Eu/NaX zeolite at 380°C. Evidence was also given that Na⁺ cations in the NaX zeolite might be considered as sites for sorption of cyclopropane and propylene (*5*).

The objective of the present work was to study the effect of Cs⁺ and Ni²⁺ ions present in NaX zeolite on the transient diffusion, sorption, and reaction of cyclopropane and propylene at 1 atm total pressure. For this, Cs⁺ and Ni²⁺ ions were exchanged for Na⁺ ions mostly in the supercages and hexagonal prisms of Zeolite X, respectively (*6–8*). Our observations support the view that Na⁺ and Cs⁺ ions might be considered sites for sorption of cyclopropane and propylene. In addi-

¹ To whom correspondence should be addressed.

tion, electrostatic fields produced by Ni^{2+} may affect sorption of these molecules in the α -cages of the Ni/NaX zeolite. The isomerization reaction of cyclopropane to propylene in the range 40–240°C was not observed in either Cs/NaX or Ni/NaX zeolites, a result opposite to that obtained with Eu/NaX (5). For the present Cs/NaX and Ni/NaX zeolites, the diluent gas used (Ar and H_2) in the $c\text{-C}_3\text{H}_6$ and C_3H_6 mixtures affects the kinetics of mass transport of these molecules in the zeolite in a manner similar to that observed with $c\text{-C}_3\text{H}_6$ in the NaX zeolite (4). The present results are discussed in relation to those obtained with NaX (4) and Eu/NaX zeolites (5). Transient and temperature-programmed methods have been employed with on-line mass spectrometry as has been reported (4, 5).

EXPERIMENTAL

Ion-exchanged zeolites. Linde NaX zeolite (600 mesh) was purchased from Alfa Ventron Corp. (Danvers, MA) and used without further purification. The crystal size was about 1.2 μm as determined by scanning electron microscopy. This material was ion-exchanged by stirring 1 g of zeolite for 18 h in a round-bottom flask with 0.05 *M* solutions of $\text{CsNO}_3 \cdot 6\text{H}_2\text{O}$ and $\text{Ni}(\text{NO}_3)_2 \cdot 6\text{H}_2\text{O}$ salts purchased from Alfa Ventron. Samples were filtered, washed with distilled deionized water, and dried under vacuum as previously described (6). The approximate formula of the exchanged zeolites are $\text{Cs}_{52}\text{Na}_{34}\text{X}$ (36 wt% Cs) and $\text{Ni}_{28}\text{Na}_{30}\text{X}$ (11.9 wt% Ni) (6, 9).

Powdered samples of 0.048–0.052 g were supported by fine stainless-steel screens and glass wool. X-ray powder diffraction results for the ion-exchanged, calcined, and treated (after sorption studies) zeolite showed that the sample retained its crystallinity (6). Prior to a transient experiment the sample was checked *in situ* for residual H_2O by mass spectrometry.

Reactor-flow system. A once-through stainless-steel microreactor (0.75 ml) was used in this study. Step change response

experiments have shown that the reactor behaves as an ideal mixed-flow reactor (CSTR) (4, 10). The flow system was the same as described earlier (10). All the lines and valves after the reactor (including the inlet capillary and ion source of the mass spectrometer) were heated to 150°C, excluding possible adsorption of cyclopropane and propylene. The pure time delay of cyclopropane and propylene response, bypassing the reactor from the switching valve to the detector, was measured as previously described (4).

Mass spectrometry/gas chromatography (GC). The high-resolution mass spectrometer (Nuclide 12-90-G), data acquisition, calibration, and integration of the mass spectrometer response have been described (11). The mass numbers (m/e) of 42, 41, and 18 were used for cyclopropane ($c\text{-C}_3\text{H}_6$), C_3H_6 , and H_2O , respectively. The composition of the effluent stream of the reactor was checked by a GC (CARLE 311) with a 1.8 m \times 2 mm stainless-steel column packed with Chromosorb 102 and an H_2 flow rate of about 25 ml/min. A flame ionization detector (FID) was used. Known dilute mixtures of $c\text{-C}_3\text{H}_6$ and C_3H_6 were prepared for calibration purposes.

Infrared spectroscopy. For the IR spectroscopic studies, the samples were pressed into thin wafers of 10 mg/cm². Dehydration of the wafer sample placed in a specially designed quartz cell was performed in a vacuum line (10^{-5} Torr) at 380°C for 12 h. After dehydration, pyridine was introduced into Cs/NaX and Ni/NaX samples by adsorption at room temperature for 10 min in a vacuum line, followed by evacuation at 120°C for 1 h. The cell was then transferred to the spectrometer and mounted there without any exposure to air. The spectrometer used was a Galaxy Series Model 4020 FTIR. The spectra were recorded as percentage transmission and obtained at room temperature.

Temperature-programmed desorption (TPD) studies. All the TPDs presented in Fig. 4, 10, and 11 were performed with Ar as a carrier gas at 1 bar pressure, a flow rate

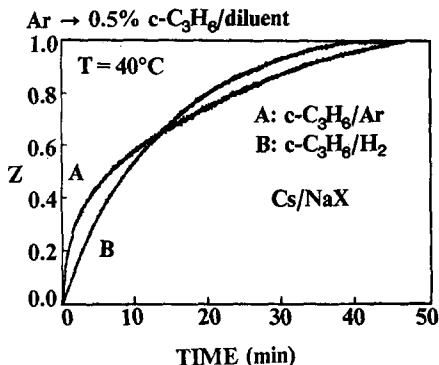


FIG. 1. Effect of diluent gas on the dimensionless gas-phase transient response (Z) of $c\text{-C}_3\text{H}_6$ in Cs/NaX . Delivery sequence: $\text{Ar} \rightarrow c\text{-C}_3\text{H}_6/\text{diluent}$. $T = 40^\circ\text{C}$; diluent gas, H_2 and Ar ; 52-mg sample used.

of 30 cc/min, and a heating rate, β , of $14^\circ\text{C}/\text{min}$. The initial amount of sorption, θ_i , was obtained by flowing 3.8 Torr of sorbate gas at 40°C over the zeolite for a given time. Before initiating the TPD, the reactor was purged with Ar at 40°C for 90 s to ensure complete removal of the sorbate in the gas phase.

Gas mixtures. Transient diffusion and reaction studies of $c\text{-C}_3\text{H}_6$ and C_3H_6 at 1 atm total pressure were performed with dilute mixtures of 0.5 mol% (3.8 Torr) sorbate gas in H_2 and Ar carrier gases. Cyclopropane and propylene were CP grade (Matheson Co.), and Ar and H_2 were zero grade (Aero All-Gas Co). Less than 2 ppm of propylene was measured by gas chromatography in the 0.5 mol% $c\text{-C}_3\text{H}_6$ mixtures, and less than 5 ppm of C_3H_8 was measured in the 0.5 mol% C_3H_6 mixtures. Argon was used in the temperature-programmed desorption studies. Purification of this gas has been described (10). The flow rate of all gases used was 30 ml/min (ambient).

RESULTS

(A) Transient Diffusion and Sorption of Cyclopropane in Cs/NaX

Transient sorption responses of $c\text{-C}_3\text{H}_6$ in dehydrated Cs/NaX zeolite (52 mg) for two different diluent gases (H_2 and Ar) at 40°C are shown in Fig. 1. The ordinate is labeled

Z , which represents the concentration (mol%) of $c\text{-C}_3\text{H}_6$ in the gas phase at some time t , $y(t)$, divided by the gas-phase concentration of $c\text{-C}_3\text{H}_6$ at equilibrium time, y_∞ , or

$$Z(t) = y(t)/y_\infty. \quad (1)$$

These data show that the gas-phase concentration of $c\text{-C}_3\text{H}_6$ rises faster (small sorption rate) at sorption times less than 15 min when Ar diluent gas is used instead of H_2 . In both cases equilibrium ($Z = 1$) is obtained after about 45 min, and the same equilibrium sorption amount (1.05 mmol/g, $Z = 1$) is obtained independent of the diluent gas used. The latter amount is calculated from the area between the mixing and sorbate gas-phase responses (11).

Data for the gas-phase response of $c\text{-C}_3\text{H}_6$ with H_2 diluent gas have been used to determine the amount of $c\text{-C}_3\text{H}_6$ sorbed in the Cs/NaX sample vs temperature. These results are given in Fig. 2 for the range $100\text{--}240^\circ\text{C}$. There is a progressively faster approach to equilibrium as the temperature is increased. Equilibrium uptake data of $c\text{-C}_3\text{H}_6$ as a function of temperature deduced from Fig. 2 are plotted in Fig. 3a. Note that the equilibrium uptake of $c\text{-C}_3\text{H}_6$ is plotted on a log scale and that this isobar is for a pressure of 3.8 Torr. The uptake data are: 0.127, 0.070,

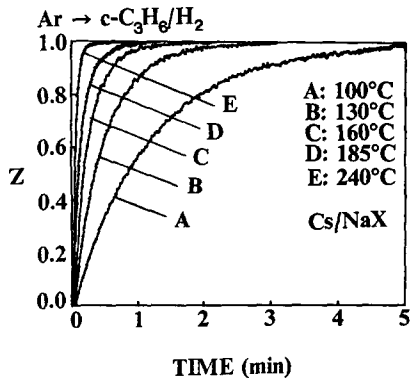


FIG. 2. Effect of temperature on the dimensionless gas-phase transient response (Z) of $c\text{-C}_3\text{H}_6$ in Cs/NaX . Delivery sequence: $\text{Ar} \rightarrow c\text{-C}_3\text{H}_6/\text{H}_2$, T ; 52-mg sample used.

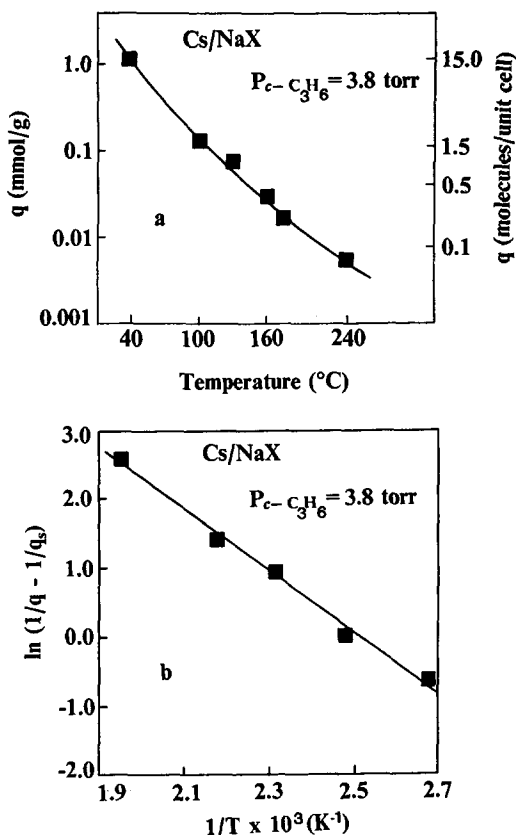


FIG. 3. (a) Equilibrium uptake of $c\text{-C}_3\text{H}_6$ (mmol/g, molecules/unit cell) vs temperature for Cs/NaX. $P_{c\text{-C}_3\text{H}_6} = 3.8$ Torr (0.5 mol%). (b) Determination of limiting values for enthalpy (ΔH^0) and entropy (ΔS^0) of sorption for $c\text{-C}_3\text{H}_6$ in Cs/NaX at 3.8 Torr based on a Langmuir model for sorption.

0.028, 0.017, and 0.005 mmol/g for 100, 130, 160, 185, and 240°C , respectively.

Thermodynamic data can be extracted from the isobar of Fig. 3a based on a Langmuir isotherm for sorption combined with the thermodynamic expression for the adsorption equilibrium constant in terms of Gibbs free energy. The resulting equation is

$$\ln(1/q - 1/q_s) = \ln(1/b_0 q_s P) + \Delta H^0/RT, \quad (2)$$

where q is the $c\text{-C}_3\text{H}_6$ uptake (molec./u.c.); q_s is the $c\text{-C}_3\text{H}_6$ uptake at saturation (molec./u.c.); and b_0 is the limiting Langmuir equilibrium constant (Torr^{-1}). ($b_0 = \exp(\Delta S^0/R)$:

ΔS^0 is the entropy of sorption (cal/mol-K), ΔH^0 is the heat of sorption (kcal/mol), and P is the pressure of $c\text{-C}_3\text{H}_6$ (Torr).) Figure 3b gives the results obtained after using the data of Fig. 3a in the range $100\text{--}240^{\circ}\text{C}$ and Eq. (2). A value of 23.9 (molec./u.c.) was used for q_s as obtained elsewhere (4). The enthalpy of sorption of $c\text{-C}_3\text{H}_6$ (ΔH^0) is found to be -8.8 kcal/mol and the entropy of sorption (ΔS^0) is -31.2 cal/mol-K.

(B) Temperature-Programmed Desorption of $c\text{-C}_3\text{H}_6$ in Cs/NaX

Temperature-programmed desorption data for $c\text{-C}_3\text{H}_6$ sorbed at 40°C and 3.8 Torr in H_2 for coverages ranging from 0.27 to 1.15 mmol/g are shown in Fig. 4. For the experiment at the lowest coverage (curve D) the temperature (T_m) at which the peak maximum occurs for the TPD is 140°C , which is the highest T_m of all the different coverages.

(C) Transient Sorption of Cyclopropane in Ni/NaX

Transient sorption responses of $c\text{-C}_3\text{H}_6$ in dehydrated Ni/NaX zeolite (48 mg) for two

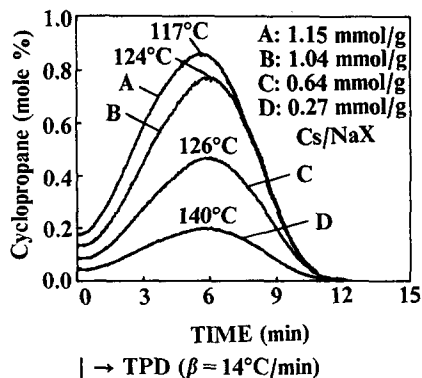


FIG. 4. TPD experiments for measuring $c\text{-C}_3\text{H}_6$ sorption in Cs/NaX. Experimental procedure: 3.8-Torr $c\text{-C}_3\text{H}_6/\text{H}_2$ (40°C , θ_i) \rightarrow Ar(90 s), 40°C \rightarrow TPD ($\beta = 14^{\circ}\text{C}/\text{min}$); 52-mg Cs/NaX. Curve A, $\theta_i = 1.15$ mmol/g; curve B, $\theta_i = 1.04$ mmol/g; curve C, $\theta_i = 0.64$ mmol/g; curve D, $\theta_i = 0.27$ mmol/g. The effect of θ_i on the peak maximum temperature T_m is also shown.

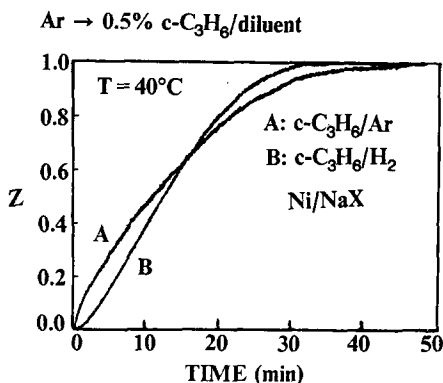


FIG. 5. Effect of diluent gas on the dimensionless gas-phase transient response (Z) of $c\text{-C}_3\text{H}_6$ in Ni/NaX. Delivery sequence: Ar \rightarrow $c\text{-C}_3\text{H}_6$ /diluent. $T = 40^\circ\text{C}$; diluent gas, H_2 and Ar; 48-mg sample used.

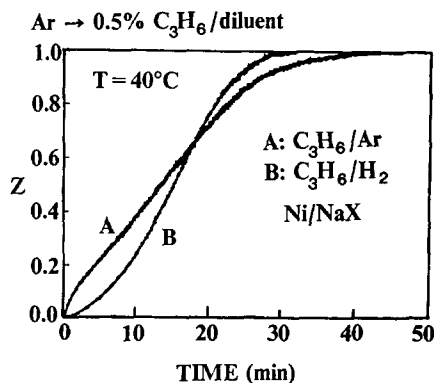


FIG. 7. Effect of diluent gas on the dimensionless gas-phase transient response (Z) of C_3H_6 in Ni/NaX. Delivery sequence: Ar \rightarrow C_3H_6 /diluent. $T = 40^\circ\text{C}$; diluent gas, H_2 and Ar; 48-mg sample used.

different diluent gases (H_2 and Ar) at 40°C are shown in Fig. 5. The effect of diluent gas on the transient mass transport of $c\text{-C}_3\text{H}_6$ in Ni/NaX is apparent. Some differences in both the responses between Ni/NaX (Fig. 5) and Cs/NaX (Fig. 1) are indicated. The equilibrium uptake ($Z = 1$) of $c\text{-C}_3\text{H}_6$ for Ni/NaX, independent of diluent gas, is found to be 1.50 mmol/g.

The effect of temperature on the transient uptake of $c\text{-C}_3\text{H}_6$ in Ni/NaX in the range $100\text{--}240^\circ\text{C}$ is given in Fig. 6 with the H_2 diluent gas. All responses reach equilibrium

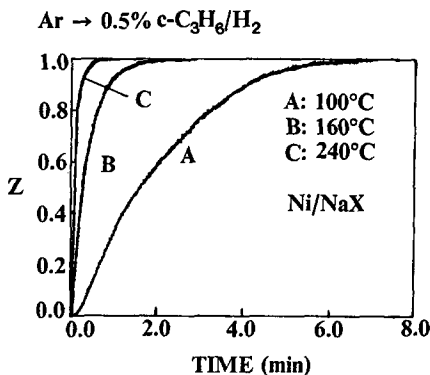


FIG. 6. Effect of temperature on the dimensionless gas-phase transient response (Z) of $c\text{-C}_3\text{H}_6$ in Ni/NaX. Delivery sequence: Ar \rightarrow $c\text{-C}_3\text{H}_6/\text{H}_2$, T ; 48-mg sample used.

($Z = 1$) in a relatively short period of time, for example, after 1 and 7 min for the temperatures of 240 and 100°C , respectively. Equilibrium uptakes of 0.252, 0.105, 0.050, and 0.010 mmol/g for 100, 130, 160, and 240°C , respectively, were measured.

(D) Transient Sorption of Propylene in Ni/NaX

A comparison of transient sorption responses of C_3H_6 to $c\text{-C}_3\text{H}_6$ in dehydrated Ni/NaX for the diluent gases of H_2 and Ar (Figs. 5 and 7) is of interest. Figure 7 gives responses of C_3H_6 for Ni/NaX at 40°C with H_2 and Ar diluent gases. In general these responses are qualitatively similar to those with $c\text{-C}_3\text{H}_6$ (Fig. 5), but some differences in the shapes of the curves can be seen. In the case of H_2 diluent equilibrium ($Z = 1$) is reached after about 30 min, whereas for Ar diluent, it is reached after about 40 min. This behavior is similar to that observed with $c\text{-C}_3\text{H}_6$ in Fig. 5. The equilibrium uptake of C_3H_6 deduced from Fig. 7 is found to be 1.85 mmol/g.

The effect of temperature on the transient response and equilibrium uptake of C_3H_6 with Ni/NaX is given in Fig. 8 in the range $130\text{--}240^\circ\text{C}$. These transient uptake responses are similar to those obtained with $c\text{-C}_3\text{H}_6$ in Ni/NaX (Fig. 6) and in Cs/NaX

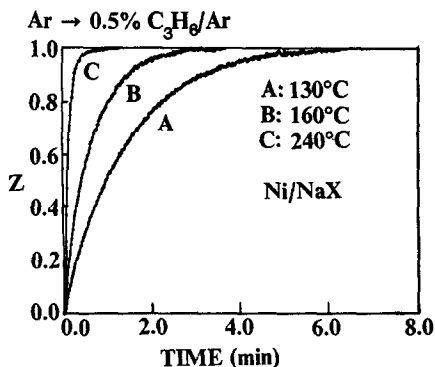


FIG. 8. Effect of temperature on the dimensionless gas-phase transient response (Z) of C_3H_6 in Ni/NaX. Delivery sequence: Ar \rightarrow $\text{C}_3\text{H}_6/\text{H}_2$, T ; 48-mg sample used.

(Fig. 2). The equilibrium amounts of C_3H_6 sorbed for the conditions of Fig. 8 are 0.170, 0.078, and 0.016 mmol/g for 130, 160, and 240°C, respectively.

Figure 9a gives the isobar at 3.8 Torr of $c\text{-C}_3\text{H}_6$ sorption in Ni/NaX zeolite in the range 40–240°C. Following the same analysis as for $c\text{-C}_3\text{H}_6$ sorption in Cs/NaX (Eq. (2), Fig. 3b), results for $c\text{-C}_3\text{H}_6$ and C_3H_6 sorption in Ni/NaX are given in Fig. 9b. The enthalpy of sorption (ΔH^0) of both $c\text{-C}_3\text{H}_6$ and C_3H_6 for Ni/NaX is found to be -9.1 kcal/mol, and the corresponding values for the entropy of sorption (ΔS^0) are -30.8 and -29.8 cal/mol-K, respectively.

(E) Temperature-Programmed Desorption of $c\text{-C}_3\text{H}_6$ and C_3H_6 in Ni/NaX

Temperature-programmed desorption data for $c\text{-C}_3\text{H}_6$ sorbed at 40°C and 3.8 Torr for coverages ranging from 0.33 to 1.50 mmol/g for given times on stream are shown in Fig. 10. Similar responses for C_3H_6 coverages ranging from 0.31 to 1.81 mmol/g are given in Fig. 11. In both cases, the same effect of initial loading of sorbate on the shift of temperature at which the maximum in the desorption rate occurred (T_M) is obtained. This effect is the increase of T_M with decreasing initial loading of $c\text{-C}_3\text{H}_6$ or C_3H_6 . On the other hand, there is a significant dif-

ference in the T_M obtained for the same initial loading of $c\text{-C}_3\text{H}_6$ and C_3H_6 . This is clearly indicated in Fig. 10, curve C, and in Fig. 11, curve D for ≈ 0.3 mmol/g, where the T_M for C_3H_6 is higher by 22°C than that for $c\text{-C}_3\text{H}_6$. For a higher initial loading (≈ 1.5 mmol/g) the same behavior is observed (compare Fig. 10, curve A, and Fig. 11, curve B).

(F) Acidity in Cs/NaX and Ni/NaX Studied by Infrared Spectroscopy

Adsorption of pyridine at room temperature in a dehydrated fresh Cs/NaX sample resulted in no infrared band at about 1540

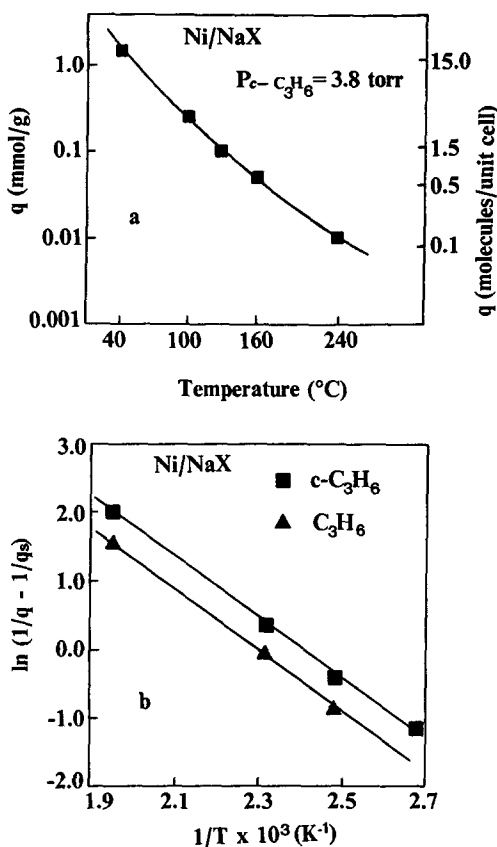


FIG. 9. (a) Equilibrium uptake of $c\text{-C}_3\text{H}_6$ (mmol/g, molecules/unit cell) vs temperature for Ni/NaX. $P_{c\text{-C}_3\text{H}_6} = 3.8$ Torr (0.5 mol%). (b) Determination of limiting values for enthalpy (ΔH^0) and entropy (ΔS^0) of sorption for $c\text{-C}_3\text{H}_6$ and C_3H_6 in Ni/NaX at 3.8 Torr based on a Langmuir model for sorption.

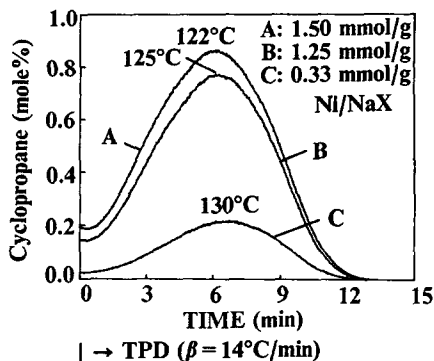


FIG. 10. TPD experiments for measuring $c\text{-C}_3\text{H}_6$ sorption in Ni/NaX. Experimental procedure: 3.8-Torr $c\text{-C}_3\text{H}_6/\text{H}_2$ (40°C , θ_i) \rightarrow Ar(90 s), 40°C \rightarrow TPD ($\beta = 14^\circ\text{C}/\text{min}$); 48-mg Cs/NaX. Curve A, $\theta_i = 1.50$ mmol/g; curve B, $\theta_i = 1.25$ mmol/g; curve C, $\theta_i = 0.33$ mmol/g. The effect of θ_i on the peak maximum temperature T_m is also shown.

cm^{-1} , the latter corresponding to the Brønsted-bound form of pyridine. On the other hand, adsorption of pyridine in a dehydrated fresh Ni/NaX sample resulted in a small band at 1548 cm^{-1} due to the presence of Brønsted acid sites.

DISCUSSION

(A) Effect of Cation in X Zeolite on the Transient Sorption of $c\text{-C}_3\text{H}_6$

An effect of diluent gas on the rate of sorption of $c\text{-C}_3\text{H}_6$ in both Cs/NaX (Fig. 1) and Ni/NaX (Fig. 5) is apparent. The data of Figs. 1 and 5 show that the initial sorption rate of $c\text{-C}_3\text{H}_6$ is greater with the diluent H_2 than with Ar. This is also true for NaX (4) and Eu/NaX (5) zeolites. Experimental evidence (4) that indicated that these $c\text{-C}_3\text{H}_6$ transient responses are only related to intracrystalline mass transport processes only was presented. Even though there are some small differences in the specific shapes of transients in Figs. 1 and 5, it is safe to say that the cations Na^+ (4), Eu^{3+} (5), Cs^+ , and Ni^{2+} have only a little influence on the diluent effect observed. On the other hand, the aforementioned cations show a pronounced effect on the equilibrium uptakes of $c\text{-C}_3\text{H}_6$.

For the case of Eu/NaX zeolite the pres-

ence of Brønsted acid sites in an amount of at least 0.6 mmol/g caused isomerization of $c\text{-C}_3\text{H}_6$ to propylene in the range $80\text{--}240^\circ\text{C}$ (5), absent in NaX zeolite (4), and an increase in the uptake of $c\text{-C}_3\text{H}_6$ at 40°C compared to NaX zeolite (4, 5). The Brønsted acidity in Eu/NaX detected by FTIR was the result of hydrolysis of $[\text{Eu}(\text{H}_2\text{O})_x]^{3+}$ ions during dehydration of the zeolite at 380°C . The $c\text{-C}_3\text{H}_6$ uptake results with Eu/NaX (5) and NaX (4) zeolites provided evidence that Na^+ cations might be considered as sites of sorption for $c\text{-C}_3\text{H}_6$.

The present equilibrium uptakes of $c\text{-C}_3\text{H}_6$ with Cs/NaX are slightly higher than the corresponding ones with NaX (4). For example, the uptake of $c\text{-C}_3\text{H}_6$ at 40°C in NaX is 1.64 mmol/g (4) compared to 1.75 mmol/g in Cs/NaX, after accounting for the difference in weight between Na^+ and Cs^+ . To probe this result let us consider what might be the effect of the polarizing power (q/r) of Na^+ and Cs^+ cations on the $c\text{-C}_3\text{H}_6$ uptake. Given the radius, r , of Na^+ and Cs^+ to be 0.97 and 1.67 \AA , respectively, and the composition of unit cells for NaX and Cs/NaX, it is calculated that the Na^+ cations in NaX create a polarizing power by a factor

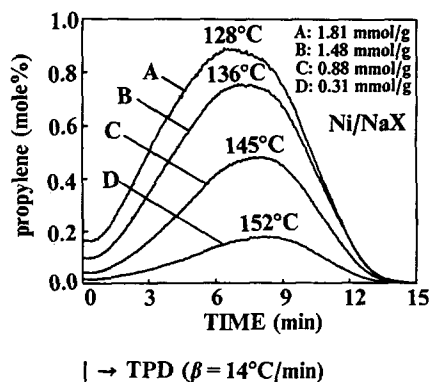


FIG. 11. TPD experiments for measuring C_3H_6 sorption in Ni/NaX. Experimental procedure: 3.8-Torr $\text{C}_3\text{H}_6/\text{H}_2$ (40°C , θ_i) \rightarrow Ar(90 s), 40°C \rightarrow TPD ($\beta = 14^\circ\text{C}/\text{min}$); 48 mg Ni/NaX. Curve A, $\theta_i = 1.81$ mmol/g; curve B, $\theta_i = 1.48$ mmol/g; curve C, $\theta_i = 0.88$ mmol/g; curve D, $\theta_i = 0.31$ mmol/g. The effect of θ_i on the peak maximum temperature T_m is also shown.

of 1.34 larger than that created by Na^+ and Cs^+ cations in the present Cs/NaX zeolite. Considering the evidence found (4) that Na^+ ions might be considered as sites for $c\text{-C}_3\text{H}_6$ sorption, the slightly higher uptake of $c\text{-C}_3\text{H}_6$ by Cs/NaX than by NaX (4) does not seem to be accounted for by electrostatic effects.

Based on the $c\text{-C}_3\text{H}_6$ sorption results at 40°C in NaX (4), a value of $3.2 \text{ Na}^+ / c\text{-C}_3\text{H}_6$ molecules is calculated, whereas for the present Cs/NaX zeolite a value of $2.9 \text{ Cs}^+ / c\text{-C}_3\text{H}_6$ molecules is calculated. These results indicate that the presence of Cs^+ ions enhance the uptake of $c\text{-C}_3\text{H}_6$ from that obtained with NaX. Spatial constraints imposed by the specific positions of Cs^+ ions in the α -cages of X zeolite, together with the appropriate orientation of $c\text{-C}_3\text{H}_6$ molecules that might be needed in order to diffuse from one α -cage to the next one, may reasonably explain the higher uptake of $c\text{-C}_3\text{H}_6$ in Cs/NaX than that in NaX zeolite.

The results of Figs. 1 and 2 with Cs/NaX show that in the range $40\text{--}240^\circ\text{C}$ equilibrium is reached ($Z = 1$). Gas chromatographic analyses revealed that no isomerization reaction of $c\text{-C}_3\text{H}_6$ to propylene had occurred. These results are consistent with the infrared results of pyridine adsorption, where no band near 1540 cm^{-1} was found, and the absence of distinct infrared -OH bands in Cs-Y zeolite (12). It is apparent that no hydrolysis of the initially hydrated Cs^+ ions that would create Brønsted acid sites occurs. Note that these sites sorb $c\text{-C}_3\text{H}_6$ at 40°C (5).

The equilibrium uptake of $c\text{-C}_3\text{H}_6$ with Ni/NaX at 40°C is 1.80 mmol/g compared to 1.64 mmol/g with NaX (4), after accounting for the difference in weight between Na^+ and Ni^{2+} . This increase in the uptake of $c\text{-C}_3\text{H}_6$ is comparable to that obtained with Cs/NaX, and this was discussed before. In the present case, however, a different explanation for this result may be appropriate. The polarizing power (per unit cell) of NaX is now about 0.8 times that of the present Ni/NaX zeolite. This result could give rise

to the observed increase in $c\text{-C}_3\text{H}_6$ uptake by Ni/NaX compared to NaX. Note that most of the Ni^{2+} ions go to the I sites inside the hexagonal prisms and also to the I' sites in the sodalite cages (7, 13), where $c\text{-C}_3\text{H}_6$ is unlikely to get into the hexagonal prisms and sodalite cages. The present infrared results of pyridine adsorption with Ni/NaX show some Brønsted acidity. This may be another cause related to the increase in uptake of $c\text{-C}_3\text{H}_6$ by Ni/NaX compared to NaX. As mentioned before, $c\text{-C}_3\text{H}_6$ can sorb on the Brønsted acid sites at 40°C (5). A reviewer has suggested that the adsorption of $c\text{-C}_3\text{H}_6$ on Ni/NaX is higher than that on Cs/NaX perhaps because Ni has vacant d orbitals but Cs does not.

The transient results of $c\text{-C}_3\text{H}_6$ with Ni/NaX in the range $100\text{--}240^\circ\text{C}$ (Fig. 6) show that equilibrium is reached ($Z = 1$), as was the case with Cs/NaX (Fig. 2), NaX (4), but not with Eu/NaX (5). Despite the fact that some Brønsted acidity is apparent from the infrared results of pyridine adsorption with Ni/NaX, 0.15 times that with Eu/NaX (5), isomerization of $c\text{-C}_3\text{H}_6$ to propylene was not observed under the present conditions. This may be consistent with the results of Bassett and Habgood (14) for Ni/NaX, where the isomerization reaction was studied at temperatures higher than 350°C .

(B) Effect of Cation in X Zeolite on the Temperature-Programmed Desorption of $c\text{-C}_3\text{H}_6$

The effect of Cs^+ and Ni^{2+} for the present zeolites on the temperature-programmed desorption of $c\text{-C}_3\text{H}_6$ in 1 atm Ar gas can be seen in Figs. 4 and 10, respectively. In both cases the peak maximum temperature, T_m , increases with decreasing initial amount of $c\text{-C}_3\text{H}_6$ sorbed (before the start of TPD). On the other hand, there is a clear indication that for the same initial amount of $c\text{-C}_3\text{H}_6$ sorbed in Cs/NaX and Ni/NaX the corresponding value of T_m is higher for Ni/NaX than for Cs/NaX. This result may be due to electrostatic fields created by Ni^{2+} that may affect sorption and desorption of $c\text{-C}_3\text{H}_6$.

On the other hand, for Eu/NaX (5) an experiment similar to that illustrated in Figs. 4 and 10 resulted in two peaks. The first peak was associated with desorption of $c\text{-C}_3\text{H}_6$ and the second peak was associated with desorption of C_3H_6 from the Brønsted sites of the Eu/NaX zeolite. The latter was the product of isomerization of $c\text{-C}_3\text{H}_6$ during the TPD.

Many factors may influence desorption of $c\text{-C}_3\text{H}_6$ from the present zeolites. Some of these factors are: cation size, intracrystalline force field, cation positions in the zeolite, and degree of ion exchange. In studying desorption and diffusion in zeolites, it is a real challenge to learn the exact contribution of each of these factors. Simulations of the $c\text{-C}_3\text{H}_6$ isothermal transients of Figs. 1, 2, 5, and 6 and those reported for NaX (4) would be more appropriate for obtaining additional information on the effects of cation on the kinetics of mass transport of $c\text{-C}_3\text{H}_6$ in Zeolite X.

Lee and Ma (15) have studied the effects of exchangeable cations on the diffusion of n -butane, isobutane, and 1-butene in Na-, Ca-, and La-forms of X zeolite. They found that the intracrystalline diffusion coefficient decreases in the order $\text{La/NaX} > \text{Ca/NaX} > \text{NaX}$. Their explanation for this result was (a) the different cation positions in the zeolite and (b) the fact that one Ca^{2+} replaces two Na^+ and one La^{3+} replaces three Na^+ , which results in a different channel opening, causing different resistances to sorbate diffusion.

(C) *Effect of Cation in X Zeolite on the Transient Sorption and Desorption of C_3H_6*

The transient uptake responses of C_3H_6 with Ni/NaX in the range 40–240°C are very similar to those obtained with NaX zeolite (5). On the other hand, the C_3H_6 transient response at 130°C with Ni/NaX (Fig. 8, curve A) is totally different from that obtained with Eu/NaX zeolite (5). The latter response was due largely to chemisorption of C_3H_6 on the Brønsted acid sites of Eu/

NaX. These results, therefore, along with those of $c\text{-C}_3\text{H}_6$ discussed before, show that Brønsted acid sites play a minor role in the interaction of C_3H_6 and $c\text{-C}_3\text{H}_6$ with the present Ni/NaX in the range 40–240°C. The C_3H_6 transient uptake responses in Figs. 7 and 8 may, therefore, be attributed mostly to the presence of Na^+ ions (5). These C_3H_6 uptakes are slightly higher than those of $c\text{-C}_3\text{H}_6$ (Fig. 3a), a result consistent with those obtained for NaX zeolite (4, 5). In addition, the C_3H_6 TPDs in Fig. 11 show higher T_m values for the same amount of sorption than the $c\text{-C}_3\text{H}_6$ TPDs in Fig. 10. These results are also consistent with the stronger interaction between C_3H_6 and Na^+ than that between $c\text{-C}_3\text{H}_6$ and Na^+ ions, probably due to the larger π -electron density of C_3H_6 .

(D) *Effect of Cation in X Zeolite on the Limiting Values of Heat and Entropy of Sorption of $c\text{-C}_3\text{H}_6$ and C_3H_6*

Figures 3b and 9b show that the Langmuir model for sorption of $c\text{-C}_3\text{H}_6$ and C_3H_6 at 3.8 Torr and in the range 100–240°C fits the experimental data very well. The same is true for the NaX zeolite (4, 5). The very low occupancy of these molecules in the zeolite crystal at the conditions studied allows calculation of limiting values for the heat and entropy of sorption of $c\text{-C}_3\text{H}_6$ and C_3H_6 (Figs. 3b and 9b, respectively). Table 1 summarizes these values for the three ion-exchanged zeolites studied, where good agreement with calorimetric values reported is obtained (1–3). Essentially, the heat of sorption for both $c\text{-C}_3\text{H}_6$ and C_3H_6 is independent of the cation used. On the other hand, the entropy of sorption does show dependence on the nature of the cation used. For example, zeolite NaX gives the lowest value for the entropy of sorption of $c\text{-C}_3\text{H}_6$ (–18.2 cal/mol-K) compared to about –30 cal/mol-K for Cs/NaX and Ni/NaX zeolites. It would be difficult to pinpoint the real causes of this behavior based only on the present results. Further results of the isosteric heats of sorption in all three zeolites

TABLE I

Limiting Values for Heat and Entropy of Sorption of Cyclopropane and Propylene in Some Ion-Exchanged X Zeolites Based on a Langmuir Isobar

Zeolite	-ΔH ⁰ (kcal/mol)		-ΔS ⁰ (cal/mol-K)		Reference
	c-C ₃ H ₆	C ₃ H ₆	c-C ₃ H ₆	C ₃ H ₆	
Na ₈₆ X	9.0	9.0	18.2	17.5	(4, 5)
Cs ₅₂ Na ₃₄ X	8.8	—	31.2	—	This work
Ni ₂₈ Na ₃₀ X	9.1	9.1	30.8	29.8	This work

studied and use of the procedure described (3) to calculate the entropy of sorption are more appropriate for shedding some light on this matter. However, this was out of the scope of the present work.

CONCLUSIONS

The following conclusions result from this work:

1. Cyclopropane and propylene sorb on Cs/NaX and Ni/NaX zeolites at 40°C with a diluent gas effect. Sorption decreases with increasing temperature but there is no reaction. Sorbed cyclopropane and propylene are recovered unchanged by temperature-programmed desorption.

2. Sorption equilibrium data for cyclopropane and propylene is Cs/NaX and Ni/NaX show good fits to the Langmuir model for sorption. The heat of sorption for these molecules is essentially independent of the Cs⁺, Ni²⁺ and Na⁺ (4) cations in zeolite X, but the entropy of sorption does depend on the nature of the cation.

3. Propylene shows a stronger interaction with Ni/NaX and NaX (4) than cyclopropane, probably because of the larger π-electron density of propylene.

ACKNOWLEDGMENT

Support of the Department of Energy, Office of Basic Energy Sciences, Division of Chemical Sciences is gratefully acknowledged.

REFERENCES

- Breck, D. W., "Zeolite Molecular Sieve." Wiley, New York, 1974.
- Barrer, R. M., "Zeolites and Clay Minerals as Sorbents and Molecular Sieves." Academic Press, New York, 1978.
- Ruthven, D. M., "Principles of Adsorption and Adsorption Processes." Wiley, New York, 1984.
- Efstathiou, A. M., Suib, S. L., and Bennett, C. O., *J. Catal.* **131**, 94 (1991).
- Efstathiou, A. M., Suib, S. L., and Bennett, C. O., *J. Catal.* **135** (1992).
- Efstathiou, A. M., Suib, S. L., and Bennett, C. O., *J. Catal.* **123**, 456 (1990).
- Smith, J. V., in "Zeolite Chemistry and Catalysis" (J. Rabo, Ed.), Vol. 171, pp. 3-78, ACS Monograph, Am. Chem. Soc., Washington, DC, 1976.
- Gallezot, P., and Imelik, B., *J. Phys. Chem.* **77**, 652 (1973).
- Stucky, G. D., Iton, L. E., Morrison, T. I., Shenoy, G., Suib, S. L., and Zenger, R. P., *J. Mol. Catal.* **27**, 71 (1984).
- Stockwell, D. M., Chung, J. S., and Bennett, C. O., *J. Catal.* **112**, 135 (1988).
- Efstathiou, A. M., and Bennett, C. O., *J. Catal.* **120**, 118 (1989).
- Uytterhoeven, J. B., Schoonheydt, R., Liengme, B. V., and Hall, W. K., *J. Catal.* **13**, 425 (1969).
- Gallezot, P., and Imelik, B., *J. Phys. Chem.* **77**, 652 (1973).
- Bassett, D. W., and Habgood, H. W., *J. Phys. Chem.* **64**, 769 (1960).
- Lee, T. Y., and Ma, Y. H., in "Molecular Sieves-II" (J. R. Katzer, Ed.), pp. 428-438, ACS Symposium Series No. 40, Am. Chem. Soc., Washington, DC, 1977.